This is the accepted manuscript made available via CHORUS. The article has been published as:

# Wave propagation in granular chains with local resonances

Luca Bonanomi, Georgios Theocharis, and Chiara Daraio

Phys. Rev. E **91**, 033208 — Published 31 March 2015

DOI: 10.1103/PhysRevE.91.033208

# Wave propagation in granular chains with local resonances

Luca Bonanomi[1], Georgios Theocharis[2,3], and Chiara Daraio[1,2]

[1] Department of Mechanical and Process Engineering (D-MAVT) ETH Zurich, Zurich, Switzerland

[2] Graduate Aerospace Laboratories (GALCIT) California Institute of Technology, Pasadena, CA 91125, USA

[3] LAUM, CNRS, Université du Maine, Avenue O. Messiaen, 72085 Le Mans, France

We study the wave propagation in a chain of spherical particles containing a local resonator. The resonant particles are made of an aluminium outer spherical shell and a steel inner mass connected by a polymeric plastic structure acting as a spring. We characterize the dynamic response of individual particles and the transmitted linear spectra of a chain of particles in contact. A wide band gap is observed both in theoretical and experimental results. We show the ability to tune the acoustic transmission by varying the contact interaction between particles. Higher driving amplitude leads to the generation of nonlinearities both in the response of a single particle and that of the whole chain. For a single resonant particle, we observe experimentally a resonant frequency downshift, which follows a complex nonlinear behaviour. In the chain of particles, nonlinearity leads to the generation of nonlinear harmonics and the presence of localized modes inside the band gap.

## I. INTRODUCTION

Artificial materials with a designed geometrical structure that supports localized resonances have been shown to present unusual behaviours with respect to electromagnetic [1] and acoustic wave propagation [2]. These media, referred to as metamaterials, give rise to many novel phenomena, including subwavelength focusing and cloaking [3, 4]. They also set the basis for the design of next-generation devices with tunable and switchable functionalities [5]. Many of these functionalities can be realized due to nonlinear processes emerging when metamaterials are excited by external stimuli [5].

In acoustics, periodic, locally resonant acoustic metamaterials [6] derive their unique properties from the presence of local resonators in the fundamental unit cells. Acoustic metamaterials have been demonstrated with periodic arrangements of coated spheres/cylinders embedded in a linear homogeneous host medium [7] and with arrays of Helmholtz resonators [8]. Currently, a great amount of work on acoustic metamaterials is devoted to the study of wave propagation in materials with near zero-density and zero-refractive-index [9-11] and nonreciprocal acoustic devices [12, 13]. Extraordinary transmission was obtained using density-near-zero ultranarrow channels [14] or through walls perforated with subwavelength holes [15]. However, in contrast to the electromagnetic counterpart, which includes numerous studies on nonlinear behaviour, research on acoustics metamaterials has been mostly limited to the linear dynamical regime.

In the realm of nonlinear acoustic crystals, a great amount of work has been devoted to the study of granular chains, which are closely packed, ordered arrangements of elastic particles (spheres in most of the cases) in contact. Due to the Hertzian contact interaction between the particles [16], the dynamic vibrational response of these structures can be nonlinear and tunable [17, 18]. This makes granular chains a perfect example for the study of fundamental phenomena

[19] and engineering applications including tunable vibration filters [20], acoustic lenses [21], and acoustic rectifiers [22].

In this work, we combine the concepts of elastic wave propagation through tunable nonlinear contacts with that of internal local resonators to design tunable, nonlinear, mechanical metamaterials. We study experimentally the response of individual resonant particles and the wave propagation through a chain of resonant particles in contact, exploring the linear and nonlinear dynamic regimes. We support the experimental findings in the linear regime with theoretical models. Similar granular chains with external resonant masses were described earlier, but their analysis was limited to the linear dynamic regime [23]. The fundamental characterization of granular chains with internal resonators is useful for their potential application in novel materials. Due to their simple geometry, particles with internal resonators are suitable to be embedded in a matrix, for example, in a composite material [24].

The rest of the manuscript is organized as follows: we describe the experimental setup in Section II. The theoretical approaches used to describe the linear behavior of the system are summarized in Section III. Section IV presents and discusses the results, and it is divided in two sub-sections: sub-section IV.A discusses the results obtained in the linearized regime and sub-section IV.B discusses results obtained at higher driving amplitude, in the nonlinear regime. Section V includes a summary of the main findings and a concluding paragraph.

## II. EXPERIMENTAL APPROACH

We fabricate the resonant particles (Fig. 1(a)) combining an outer mass (a spherical shell), an inner mass (a solid sphere) and an elastic structure between the two. The outer mass is an aluminum hollow shell (alloy 3003, diameter = 18.6 mm, wall thickness = 0.8 ± 0.1 mm, mass, $m_1$ = 2.3 ± 0.05 g, Young's modulus = 69 GPa, Poisson's ratio = 0.33). The inner mass consists

of a solid stainless steel bead (316 type, diameter = 12.8 mm, $m_2 = 8.6 \pm 0.1$ g, Young's modulus = 193 GPa, Poisson's ratio = 0.3). The reported values of Young's moduli and Poisson's ratios are standard specifications [25]. The elastic structure (spring) connecting the two masses is made of a commercial plastic (*Verowhite Plus*, by Stratasys$^{TM}$) having a Young's modulus of 2500 MPa [26] and a mass of 0.2 g. The shape of the elastic spring is shown in Fig. 1(a) and was fabricated by 3D printing (in a Stratasys$^{TM}$ Object Connex 500).

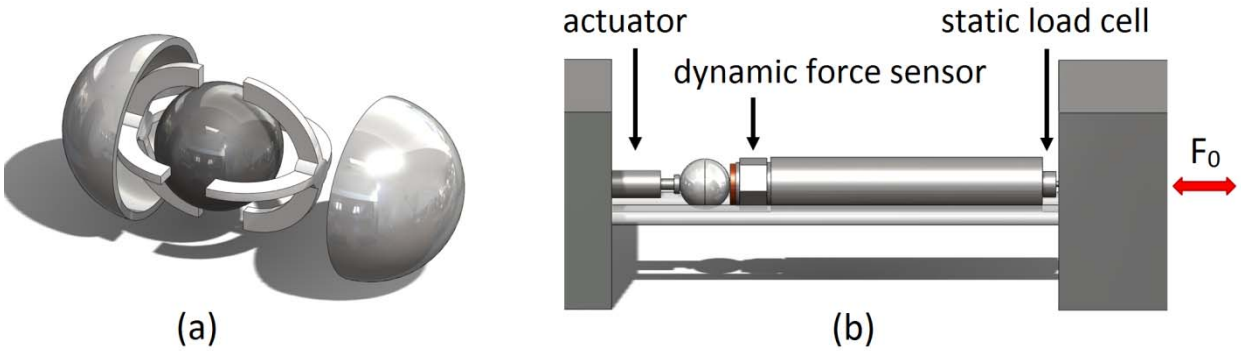


FIG. 1. (a) Parts and assembly of a resonant unit cell. (b) Schematic of the experimental setup to test the dynamic response of a single particle.

To test the dynamic response of a single particle and that of a chain of particles in contact, we align and hold the particle(s) in a support system consisting of four polycarbonate rods, held in place by polycarbonate guide plates [20]. An initial static compression is applied on one side by using a translating steel cube. The static force applied is measured with a piezoelectric static load cell (Fig. 1(b)). We continuously drive the particle(s) with a piezo-electric actuator mounted on a fixed steel cube, on the opposite side with respect to the static force sensor. We record the transmitted force-time history using a dynamic force sensor. The input signal and the transmitted signal are generated and measured using a lock-in amplifier. A

heavy steel cylinder is added to the system in order to measure simultaneously the dynamic force and the static load.

The linear regime is explored exciting the system with low amplitude (approximately 10 mN peak) swept sine signal from 0.5 to 20 kHz. We compute the power spectral density (PSD) of the signal collected by the dynamic force sensor. Increasing the excitation amplitude (up to approximately 0.5 N peak) it is possible to investigate the nonlinear regime, as shown in the results and discussion section.

## III. THEORETICAL APPROACH

The nonlinear interaction law between two elastic particles is well described by the Hertzian contact law [16]. In Hertzian contacts, the contact force $F_{i,i+1}$ between two particles ($i$ and $i+1$) relates to the relative displacement $\Delta_{i,i+1}$ of their particles' centers, as:

$$F_{i,i+1} = A_{i,i+1}[\Delta_{i,i+1}]_+^{n_{i,i+1}} \qquad (1).$$

Here, $A_{i,i+1}$ and $n_{i,i+1}$ depend on the geometry and material properties of the particles in contact. Values inside the bracket $[s]_+$ only take positive values, which denotes the tensionless characteristic of the system (i.e., there is no force between the particles when they are separated). The contact interaction between thin hollow spheres was studied in [27]. For the range of wave amplitude considered in [27], a power-law type relation ($F=k\delta^n$) was also used to describe the contact. It was found, however, that the exponent $n$ was smaller than the value 3/2 found in the classical Hertzian interaction between solid spheres. The contact stiffness $k$ and the exponent $n$ were found to be dependent on the thickness of the hollow sphere's shell [27]. This dependence of the contact stiffness on the shell thickness can be used in the design of particles-based metamaterials to tune their resulting transmission spectrum.

The characteristic dynamic response of a single resonant particle compressed between two fixed walls (representing the actuator and the dynamic force sensor in the experimental setup) is expected to present two resonances, corresponding to the in-phase (at lower frequency) and to the out-of-phase (at higher frequency) motion of the outer and inner masses. Ignoring dissipation, these eigenfrequencies are given by:

$$f_{1,2} = \frac{1}{2\pi}\sqrt{\frac{2k_0m_2+k_2(m_1+m_2)\pm\sqrt{-8k_0k_2m_1m_2+[2k_0m_2+(m_1+m_2)k_2]^2}}{2m_1m_2}} \quad (2).$$

Here $k_0$ describes the linearized contact stiffness [28] between the outer shell and the steel wall, while $k_2$ represents the effective stiffness of the inner spring. To describe the dynamics of the locally resonant granular chain considered in this work, we adopt a lumped-element numerical approach. The validity of this approach is based on the fact that for the applied frequency range (0.5-20 kHz), collective resonant vibrations of the individual parts of the resonant unit cells are not excited. In order to verify this assumption, we computed the vibrational analysis of each part of a resonant sphere using a finite element model (COMSOL Multiphysics) finding that every resonant mode is above 30 kHz. Thus, the system can be considered as a mass-in-mass lattice [29] and its linear response is described by the following equations of motion [28]:

$$\begin{aligned} m_1\ddot{u}_1^{(j)} &= k_1\left(u_1^{(j-1)} - 2u_1^{(j)} + u_1^{(j+1)}\right) + k_2\left(u_2^{(j)} - u_1^{(j)}\right) + \eta\left(\dot{u}_2^{(j)} - \dot{u}_1^{(j)}\right) \\ m_2\ddot{u}_2^{(j)} &= k_2\left(u_1^{(j)} - u_2^{(j)}\right) + \eta\left(\dot{u}_1^{(j)} - \dot{u}_2^{(j)}\right), \end{aligned} \quad (3)$$

where $u_{1,2}^{(j)}$ represents the displacement of mass "*1,2*" in the $j^{th}$ cell. The elastic structure, being much softer of the two masses, plays the role of a linear, damped spring with an effective stiffness $k_2$ and a viscous damping coefficient $\eta$. We assume that most of the dissipation in our physical system occurs inside each unit (introduced by the polymeric structure connecting the shell with the inner mass) and not in the contact between two units. Finally, $k_1$ is the equivalent

of $k_0$ (linearized contact stiffness) between the outer shells of two resonant spheres and depends on the static precompression $F_0$ as $k_1 = nA^{\frac{1}{n}}F_0^{\frac{n-1}{n}}$.

The dispersion relation of an infinite chain of resonant particles presents two bands of propagating frequencies (acoustic and optical) separated by a band gap. For the loss-less case ($\eta=0$) the positions of the band edges are given by the following analytical values (the acoustic band starts from 0):

$$f_1 = 1/(2\pi)\ [(b-(b^2-4ac)^{1/2})/2a)]^{1/2},$$

$$f_2 = 1/(2\pi)\ [k_2(m_1+m_2)/(m_1m_2)]^{1/2},$$

$$f_3 = 1/(2\pi)\ [(b+(b^2-4ac)^{1/2})/2a)]^{1/2}, \qquad (4)$$

where $a = m_1m_2$, $b = k_2(m_1+m_2)+4m_2k_1$ and $c = 4k_1k_2$. The upper acoustic edge $f_1$ and the upper optical edge $f_3$ depend on $k_1$ and thus on the static load. The contact stiffness $k_1$ changes with the precompression ($F_0$). This is an important feature of granular chains and allows tuning their transmission spectrum by the application of a (variable) external force [20, 30].

## IV. RESULTS AND DISCUSSION

### A. Linear regime

To extract the physical parameters to be used in our numerical model, we first measure the acoustic properties of a single resonant particle (Fig. 2).

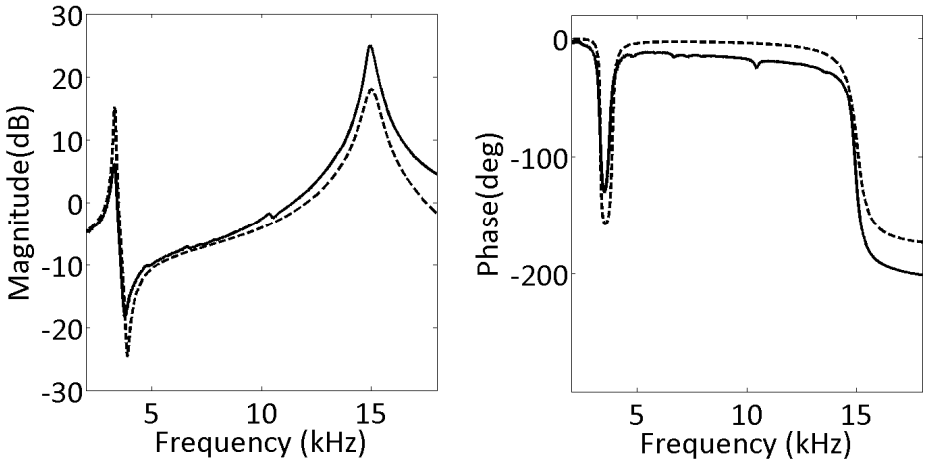


FIG. 2. Experimental (solid line) and numerical (dashed line) magnitude (a) and phase (b) of the transfer function of a single resonant particle in the linear regime.

From Eq. (2) and the experimental vibrational peaks of a single resonant sphere under a static load of $F_0$=17.3 N (Fig. 2a), we extract the linearized contact stiffness between the aluminum spherical shell and a stainless flat surface (actuator and force sensor) $k_0$, and $k_2$. The values obtained from the fitting are $k_0 = 7.5 \cdot 10^6$ N/m and $k_2 = 5.1 \cdot 10^6$ N/m. Considering a power law contact interaction ($F=A\delta^n$) and various static loads, we find that $n$=1.154 and $A=4.583 \cdot 10^7$ N/m$^{(n)}$. Finally, we estimate the dissipation coefficient, $\eta$ = 8.6 kg/s, measuring the quality factor (and damping coefficient $\tau$) of the out-of-phase resonant peak.

The results reported in Figs. 2(a),(b) show a very good agreement between the experimental and the numerical transfer function obtained using the state-space approach [31]. This proves the validity of the lumped-element approach. A better agreement could be obtained using a more sophisticated modeling of the viscoelastic dissipation, but this is out of the scope of the present work. The transmission dip observed at $f_0$=3.8 kHz corresponds to an anti-resonance around which the dynamic mass density displays a resonance-like behavior (see chapter 5 of [2]).

At that frequency, the displacement amplitude of the outer mass $m_1$ becomes zero as a result of a destructive interference of oscillations from the driver and the $m_2$ oscillator (the oscillations of the driver and the $m_2$ are out-of-phase). This is confirmed by the fact that $f_0=1/(2\pi)(k_2/m_2)^{1/2}$.

From the experimental acoustic response of two resonant unit cells, we derive the parameters for the fundamental contact law between the spherical shells ($F=A\delta^n$). We find that $n$ = 1.245 and $A = 7.4\cdot10^7$ N/m$^{(n)}$. These values are in good agreement with those obtained above and with finite element methods (FEM) in [27].

Using the Bloch state-space formulation (see chapter 6 of [2]) and the experimental parameters, we derive the damped frequency band structure, Fig. 3(a), and the corresponding wavenumber-dependent damping ratio, Fig 3(b), for the infinite chain case. The existence of a band gap is clear (Fig 3 (a)). The origin of this gap is connected with hybridization effects of the dispersion curve of a monoatomic chain of particles with the local resonances. The lower (upper) pass bands consist of modes where the inner and outer masses are oscillating in-phase (out-of-phase). From Fig 3 (b), we can conclude that the damping ratio of the optical branch modes is higher than that of the acoustic modes, since the presence of the damping material (the 3D printed polymeric structure) influences mostly the out-of-phase motion of the two masses. Among the optical modes, the ones with lower wavenumber experience higher drop rates. Comparing the analytical expressions of the band edges and the damped frequency band structure, we can conclude that the presence of the dissipation has no influence on the dispersive properties of the structure. In Fig. 3 (c), we show the numerical transfer function for a chain consisting of 11 locally resonant units, with two different initial static loads.

We characterize the linear behavior of the same system using experiments (Fig. 3(d)). We note that, for a static load of 22.6 N, a wide band gap exists between $f_1$=3.5 kHz and $f_2$=8 kHz as well as a gap above $f_3$=17 kHz. We obtain a very good agreement between experiments (Fig.

3(d)), numerical results (Fig. 3(c)) and theory (vertical lines in Figs. 3(c) and 3(d)). To validate that it is possible to tune the band frequencies by varying the static precompression also in experiments, we decreased the static preload from 22.6 N to 12.6 N. In this case, the upper cut-off frequency of the optical band downshifts of about 1 kHz, while the upper acoustic edge and the lower optical edge shift only a few Hz (not possible to resolve in experiments). The dip around 11 kHz, which is not captured by the theoretical model, comes from the cavity resonance of the air contained within the resonant particle (computed and verified using finite element model (COMSOL Multiphysics)).

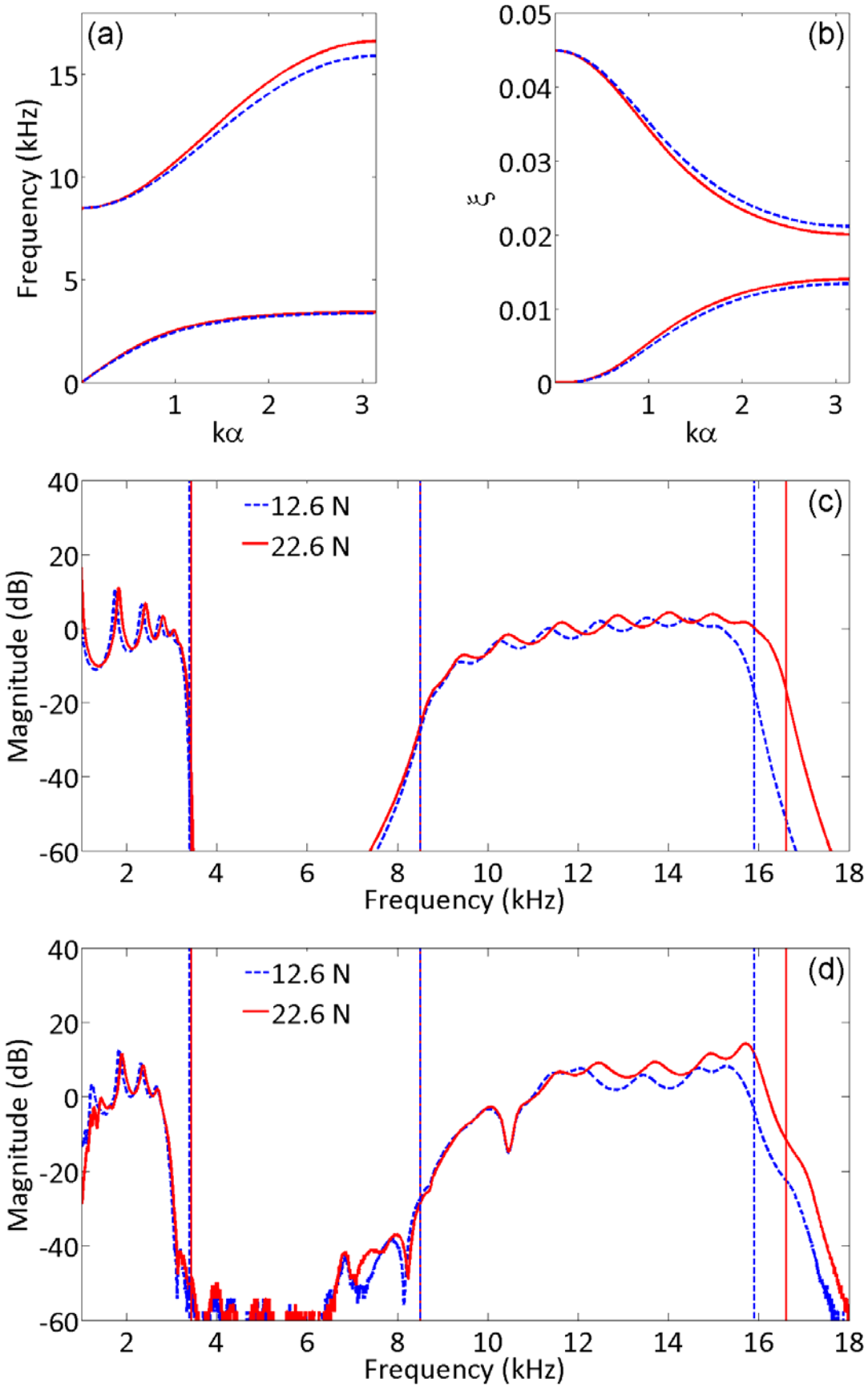
(a)
Frequency (kHz)
kα
(b)
ξ
kα
(c)
12.6 N
22.6 N
Magnitude (dB)
Frequency (kHz)
(d)
12.6 N
22.6 N
Magnitude (dB)
Frequency (kHz)

FIG. 3. (a) Damped dispersion relation for an infinite 1D locally resonant granular chain using the experimentally obtained parameters (k is the wavenumber and α is the length of one unit). (b) Damping ratio band structure for $F_0$=22.6 N (solid lines) and $F_0$=12.6 N (dotted line) respectively. (c) Numerical magnitude of the transfer function for two different pre-compression values. (d) Experimental transfer function of a chain of 11 resonant particles under the applied load of 22.6 N (solid line) and 12.6 N (dotted line). The vertical lines in panel (c) and (d) denote the analytical values of the frequencies of the band edges from Eq. (4).

**B. Nonlinear regime**

We also explore in experiments the nonlinear dynamics of our structure by increasing the amplitude of the driving excitation up to approximately 0.1 N peak. The response of a single resonant particle for different amplitudes of the input signal is shown in Fig. 4. Fig. 4(a) shows the frequency shift of the first resonance (the one corresponding to the in-phase motion of the two masses), while Fig. 4(b) shows the same results for the second resonance (the one corresponding to the out-of-phase motion of the two masses). Experiments clearly show that a softening effect emerges for both resonances, when the driving amplitude is increased. This softening effect is a well-known nonlinear phenomenon but, according to the prediction of a simple phenomenological model (e.g., the Duffing oscillator) [32] and in accordance with the response reported for weakly nonlinear Hertzian nonlinearity [33], the resonance frequency shift $\Delta f$ should follow a quadratic softening as a function of the drive amplitude. However, in our experiments, both resonances follow a linear dependence on the amplitude (Fig. 4(c) and 4(d)). The dotted lines in Fig. 4(c) and 4(d) show the numerical nonlinear resonance shift obtained using Eq. (3) combined with the nonlinear force model described in Eq. (1). In these calculations, we assumed the inner springs to be linear and, in agreement with earlier theoretical work on granular chains [33], we obtain a quadratic softening. A linear amplitude dependence is

commonly observed in a wide class of materials called mesoscopic media [34, 35], including damaged solids and geomaterials, and is attributed to hysteretic quadratic nonlinearity. In the case of granular media, it has been shown that frictional nonlinearities (for example the single shear contact between two spheres) exhibit nonlinear hysteresis [36]. In our case, the hysteretic nonlinear response of the two resonant modes is induced by the presence of the soft elastic spring. Nonlinear hysteretic mechanisms can originate from the complex, frictional contact forces between the elastic structure with the outer shell and the inner mass, and from other mechanisms such as thermoelastic or viscous losses [37, 38]. These effects could explain the linear amplitude-dependent frequency downshift observed. The same mechanisms could also explain the weak, amplitude-dependent variation of dissipation mostly evident in the out-of-phase resonance. To capture the experimental response correctly, a more sophisticated modeling of the nonlinear response of the soft elastic spring and the inner contacts would be needed. For example, mesoscopic approaches like the Preisach-Mayergoyz space [34], could be used to describe the hysteretic nonlinear dynamics of the proposed structure.

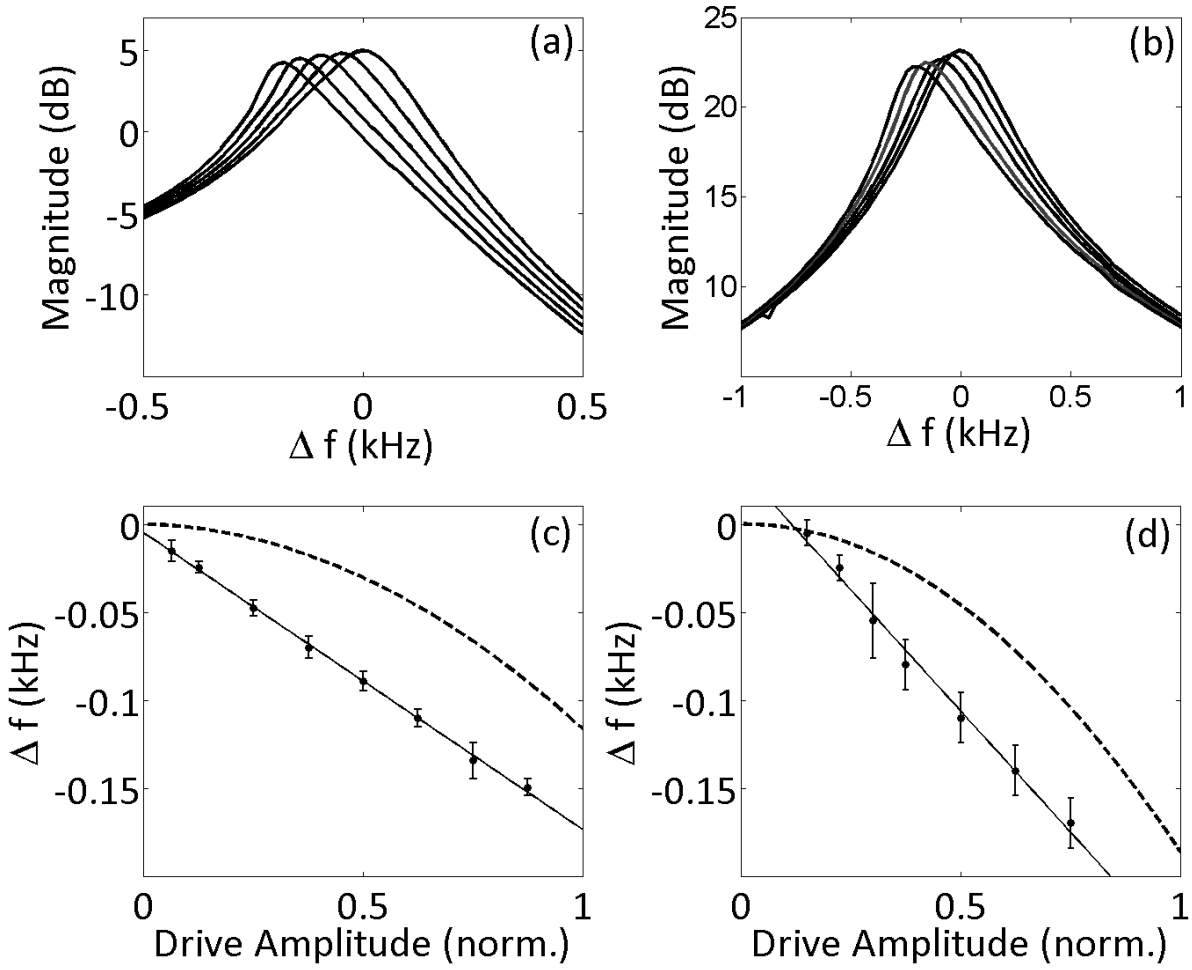


FIG. 4. (a) Experimentally measured acoustic transfer function for the in-phase motion and (b) for the out-of-phase motion. (c) Resonance frequency shift as a function of the drive amplitude for the in-phase motion resonance and (d) for the out-of-phase motion resonance. Marks and error bars are the average and the standard deviation from a set of 3 measurements. Dotted lines in (c) and in (d) show the simulated shift without considering nonlinearities for the inner spring.

We also study the nonlinear dynamics of a chain of resonant particles. We drive the chain with a signal composed of a low amplitude (approximately 10 mN peak) sine waves swept between 1 kHz and 17 kHz. To trigger a nonlinear response we superimpose to this low amplitude signal a large amplitude wave (approximately 0.5 N peak) at a fixed frequency (1.68 kHz). This high

amplitude driving frequency is chosen to be within the acoustic band. The transmitted signal recorded at the end of the chain shows the generation of the second and third harmonics in the band gap. These harmonics are located within the band gap and for this reason they are evanescent, thus they do not accumulate with distance nor propagate. However, since the fundamental harmonic (the one generated by the harmonic driving) is in the acoustic band, it can propagate along the chain and reach the end of the chain. The signal detected by the force sensor contains evanescent modes, localized at the end of the chain, forced by the fundamental harmonic wave, which plays the role of a nonlinear source. Thus, driving the system at high amplitude within the acoustic band is a way to transmit a signal at a frequency inside the band gap. As in the analysis of single resonant particles, we numerically solve the equations of motion taking into account the fully nonlinear contact forces and considering the inner forces to be linear. The high amplitude driving signal in the numerical study has been chosen to match the frequency of one of the resonant modes contained in the acoustic band. Fig. 5 shows the transmitted signal obtained numerically (Fig. 5(a)) and experimentally (Fig. 5b). It is important to note that a high amplitude input signal at a frequency inside the band gap is not detected at the end of the chain, both in experiments and in simulations; this is an additional proof of the good filtering features of the proposed system.

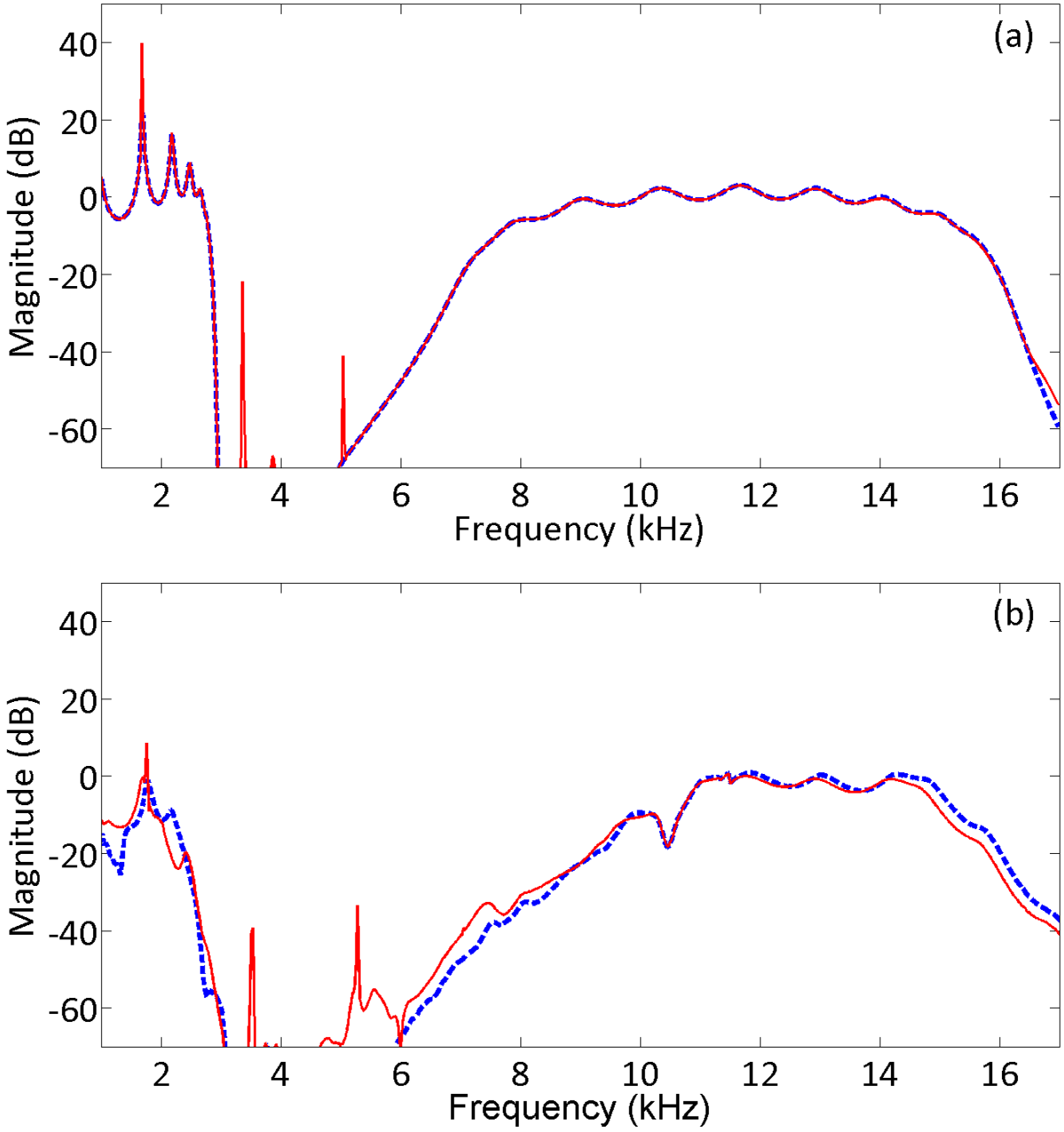


FIG. 5. Red solid lines represent the magnitude of the transfer function (a) simulated and (b) measured experimentally, when a chain of resonant particles was driven with a high amplitude (approximately 0.5 N peak) harmonic signal at 1.68 kHz, superimposed to a swept since frequency at low amplitude (approximately 10 mN peak). Blue dotted lines in both panels show the magnitude of the transfer function without the high amplitude signal.

From the results, it is evident that harmonic signals with a frequency within the band gap can be detected at the end of the chain if the system enters the nonlinear regime. The nonlinear properties of the presented chain lead also to amplitude-dependent transmitted spectra.

## V. CONCLUSIONS

We designed and built a chain of granular elements containing internal resonators and we characterized it using experiments and theoretical approaches. The local resonances resulted in the existence of a wide band gap in the audible regime that makes the system capable of filtering mechanical waves between 3 and 8.5 kHz and above 17 kHz. This frequency range can be tuned by ~1 kHz varying the static precompression applied on the chain. We have characterized the dynamics of the compressed 1D chain using theory, numerical simulations and experiments finding good agreement for the linear spectrum. We explored the nonlinear dynamic regime in experiments. In a single resonant particle, the presence of the internal spring leads to a nonlinear dynamic behaviour. In a chain of resonant particles, the presence of nonlinearities leads to harmonics generation inside the band gap. Our experimental results provide a first demonstration of a practical way to use nonlinearity as a way to tune the dynamic properties of acoustic metamaterials. Thanks to their simple geometry, our systems could easily be embedded in a matrix, providing the basis to create novel materials for vibration mitigation and impact absorption.

## ACKNOWLEDGMENTS

L.B. and C.D. acknowledge support from the US NSF, grant number 0969541 and the US Office of Naval Research, YIP program. They also acknowledge partial support from the Army

Research Office MURI grant US ARO W911NF-09-1-0436. G.T. acknowledges support from CIG FP7 ComGranSol. We thank Marc Serra Garcia for his support in experiments, and V. Tournat and D. Ngo for helpful discussions.

## References

[1] L. Solymar and E. Shamonina, *Waves in Metamaterials* (Oxford University Press Inc., New York, 2009), Chap. 9, p. 289-309.
[2] P. A. Deymier (Ed.), *Acoustic Metamaterials and Phononic Crystals* (Springer-Verlag Berlin Heidelberg, 2013), Chap. 6-7, p. 201-252.
[3] T. J. Cui, D. Smith, and R. Liu (Eds.), *Metamaterials: Theory, Design and Applications* (Springer Science+Business Media LLC, New York, 2010), Chap. 6 and 8, p. 99-114 and 155-180.
[4] R. V. Craster and S. Guenneau (Eds), *Acoustic Metamaterials* (Springer Science+Business Media, Dordrecht, 2013), Chap. 6 and 9, p. 141-168 and 219-240.
[5] N. I. Zheludev and Y. S. Kivshar, Nat. Mater., **11**, 917 (2012).
[6] M. -H. Lu, L. Feng, and Y. -F. Chen, Materials Today, **12**, 34 (2009).
[7] Z. Liu, X. Zhang, Y. Mao, Y. Y. Zhu, Z. Yang, C. T. Chan, and P. Sheng, Science, **289**, 1734 (2000).
[8] N. Fang, D. Xi, J. Xu, M. Ambati, W. Srituravanich, C. Sun, and X. Zhang, Nat. Mater., **5**, 452 (2006).
[9] Z. Liang and J. Li, Phys. Rev. Lett., **108**, 114301 (2012).
[10] C. M. Park and S. H. Lee, Appl. Phys. Lett., **102**, 241906 (2013).
[11] L. Y. Zheng, Y. Wu, X. Ni, Z. -G. Chen, M. -H. Lu, and Y. -F. Chen, Appl. Phys. Lett., **104**, 161904 (2014).
[12] R. Fleury, D. L. Sounas, C. F. Sieck, M. R. Haberman, and A. Alù, Science, **343**, 516 (2014).
[13] B. -I. Popa and S. A. Cummer, Nat. Commun., **5**, 3398 (2014).
[14] R. Fleury and A. Alù, Phys. Rev. Lett., **111**, 055501 (2013).
[15] J. J. Park, K. J. B. Lee, O. B. Wright, M. K. Jung, and S. H. Lee, Phys. Rev. Lett., **110**, 244302 (2013).
[16] K. L. Johnson, *Contact Mechanics* (Cambridge University Press, 1985).
[17] V. F. Nesterenko, *Dynamics of Heterogeneous Materials* (Springer-Verlag, New York, 2010), Chap. 1, p. 1-136.
[18] C. Daraio, V. F. Nesterenko, E. B. Herbold, and S. Jin, Phys. Rev. E, **73**, 026610 (2006).
[19] Y. Man, N. Boechler, G. Theocharis, P. G. Kevrekidis, and C. Daraio, Phys. Rev. E, **85**, 037601 (2012).
[20] N. Boechler, J. Yang, G. Theocharis, P. G. Kevrekidis, and C. Daraio, J. Appl. Phys., **109**, 074906 (2011).
[21] A. Spadoni and C. Daraio, PNAS, **107**, 7230 (2010).
[22] N. Boechler, G. Theocharis, and C. Daraio, Nat. Mater., **10**, 665 (2011).
[23] G. Gantzounis, M. Serra-Garcia, K. Homma, J. M. Mendoza, and C. Daraio, J. Appl. Phys., **114**, 093514 (2013).
[24] S. J. Mitchell, A. Pandolfi, and M. Ortiz, J. Mech. Phys. Solids, **65**, 69 (2014).
[25] *Metals Handbook, 10th ed.* (ASM International, Materials Park, OH, 1990).
[26] http://www.stratasys.com.
[27] D. Ngo, S. Griffiths, D. Khatri, and C. Daraio, Granul. Matter, **15**, 149 (2013).
[28] G. Theocharis, M. Kavousanakis, P. G. Kevrekidis, C. Daraio, M. A. Porter, and I. G. Kevrekidis, Phys. Rev. E, **80**, 066601 (2009).
[29] H. H. Huang and C. T. Sun, New J. Phys., **11**, 013003 (2009).

[30] E. B. Herbold, J. Kim, V. F. Nesterenko, S. Y. Wang, and C. Daraio, Acta Mech, **205**, 85 (2009).
[31] K. Ogata, *System Dynamics, 4th ed.* (Prentice-Hall, Upper Saddle River, NJ, 2004).
[32] J. A. TenCate, D. Pasqualini, S. Habib, K. Heitmann, D. Higdon, and P. A. Johnson, Phys. Rev. Lett., **93**, 065501 (2004).
[33] J. Cabaret, V. Tournat, and P. Béquin, Phys. Rev. E, **86**, 041305 (2012).
[34] R. A. Guyer, J. TenCate, and P. Johnson, Phys. Rev. Lett., **82**, 3280 (1999).
[35] R. A. Guyer and P. A. Johnson, Phys. Today, **52**, 30 (1999).
[36] R. D. Mindlin and H. Deresiewicz, J. Appl. Mech., **20**, 327 (1953).
[37] L. Filinger, V.Y. Zaitsev, V. Gusev, and B. Castagnède, Acta Acust. Acust., **92**, 24 (2006).
[38] V.Y. Zaitsev and P. Sas, Acta Acust. Acust., **86**, 429 (2000).